



Title	CHARACTERISTICS OF SODIUM CHLORIDE-DOPED SILVER CATALYSTS FOR EPOXIDATION OF ETHYLENE
Author(s)	AYAME, Akimi; MIURA, Hiroyuki; KIMURA, Tetsuo; YAMAGUCHI, Masatsugu; KANO, Hisao; MIYAHARA, Koshiro; TOYOSHIMA, Isamu
Citation	JOURNAL OF THE RESEARCH INSTITUTE FOR CATALYSIS HOKKAIDO UNIVERSITY, 32(2/3), 49-64
Issue Date	1985-03
Doc URL	http://hdl.handle.net/2115/28064
Type	bulletin (article)
File Information	32(2_3)_P49-64.pdf



[Instructions for use](#)

CHARACTERISTICS OF SODIUM CHLORIDE-DOPED SILVER CATALYSTS FOR EPOXIDATION OF ETHYLENE

By

Akimi AYAME,^{*)} Hiroyuki MIURA,^{*)} Tetsuo KIMURA,^{*)}
Masatsugu YAMAGUCHI,^{*)} Hisao KANO,^{*)}
Koshiro MIYAHARA^{**)} and Isamu TOYOSHIMA^{**)}

(Received January 13, 1984)

Abstracts

Catalytic activity and selectivity of NaCl-doped Ag catalysts and granular NaCl-supported Ag catalysts for the epoxidation of ethylene were examined by a pulse technique. On both catalysts with the same NaCl content, no noticeable differences in activity were found. Increasing amounts of NaCl, while slightly reduces the activity expressed in terms of total catalyst mass, however increases it when referred to the weight of Ag. The ethylene oxide concentration in the gaseous products is 97~99% in all cases. However, the net selectivity is estimated to be less than 86%, since the carbon-containing species remained irreversibly during the reaction are converted to carbon dioxide and water. The catalysts are almost inactive for the oxidation of ethylene oxide.

XRD measurements reveal that the reduced catalyst contains solely Ag and NaCl. Further, AES and XPS studies suggest that Na and Cl atoms are concentrated in the surface layers accompanying by subsurface oxygen atoms, and Ag, Na, and Cl form their peculiar ionic states by the strong interactions among all elements including oxygen, because their band structures are distorted.

Introduction

The first description for the direct oxidation of ethylene to ethylene oxide over silver catalysts is found in a patent in 1931¹⁾. Since then, many fundamental studies relating to the catalyst preparation, oxygen adsorption, kinetics, and catalyst deactivation have been performed, and are then summarised in many review articles.^{2,3)} The selectivity to ethylene oxide in the first commercial process in 1947 was 55%.⁴⁾ In recent years, high-selective catalysts have been developed and then a new effective process is also

*) Department of Industrial Chemistry, Muroran Institute of Technology, Muroran, 050 Japan.

**) Research Institute for Catalysis, Hokkaido University, Sapporo 060, Japan.

established.⁵⁾ In the course of these developments, a remarkable increase of 25~27% in selectivity has been achieved. The selectivity has been improved by doping one or more alkali or alkaline earth metals to the silver catalyst and by adding trace amounts of chlorine or chlorinated organic compounds to the feed gas. Kilty and Sachtler³⁾ demonstrated that chlorine retards the dissociative adsorption of oxygen on silver surface so as to increase the selectivity. Other authors⁶⁻⁸⁾ have also suggested similar role for chlorine in achieving higher selectivity. It was reported that the addition of alkaline earth metals decreases the work function of the catalyst surface by covering silver surface with semiconducting film involving silver atoms as electron donors.⁹⁾ Further, alkali metals as well as silver are well known to form super-oxides (MO_2).¹⁰⁾

In the present context of effective uses of carbon-containing resources, the selectivity of 80~82% mentioned above is not sufficient for commercial epoxidation processes. The present authors have recently reported that the simultaneous addition of sodium and chlorine-containing compounds to silver was very effective.¹¹⁾ In the present work, we examined the catalytic capability of the fresh NaCl-doped silver catalysts and granular NaCl-supported silver catalysts for the epoxidation of ethylene using a pulse technique. Further, the change of bulk composition of the catalyst with hydrogen reduction was measured using XRD and the catalyst surface was characterized by AES and XPS.

Experimental

Catalyst Preparation and Materials

All chemicals employed were commercially available reagents of high purity (supplied by Kanto Chem. Co.) and were used without further purification. Ag_2O was prepared from 2N-aqueous solution of AgNO_3 and KOH . About 100 g of the precipitated Ag_2O was, after filtration, washed with about 60 ℓ of twice-distilled H_2O for a period of 5 days, and dried in an oven at 383 K for 20 h. In a glove box purged continuously with N_2 gas, the dried Ag_2O was mixed with an aqueous solution of NaCl in an evaporating ceramic dish. The resulting mixture was dried on a hot plate at 373~383 K. The mixture was immediately transferred into a U-type glass tube and reduced first at 333 K for 20 h in a stream of H_2 . Then the reduction temperature was elevated at a rate of 50 K/20 min and finally kept at 673 K for 10 h. The reduced catalyst was ground to a powder of more than 150 mesh in the glove box and preserved in a glass tube purged with H_2 or inert gas. Granular NaCl-supported Ag catalysts were prepared by the

Characteristics of Silver Catalysts

following method: the Ag_2O , which was pasted with distilled $\text{C}_2\text{H}_5\text{OH}$, was mixed well with granular NaCl and $\text{C}_2\text{H}_5\text{OH}$ was then vaporized slowly in the glove box. The subsequent operations were performed by employing the same procedures as used for the preparation of the doped powdered catalyst. After reducing and annealing the supported catalyst at 673 K for 10 h, no particle separation of Ag and NaCl was observed without vigorous handling.

Commercial C_2H_4 (99.9%) and O_2 (99.8%) were used to prepare reactant mixtures, after they were purified by distillation twice in a vacuum system. He (99.9999%) was used as a carrier gas and diluent after passing through a Oxisorb column. H_2 (99.9%) and N_2 (99.8%) were passed through silica gel columns.

Apparatus

Activity and selectivity were measured using a pulse reactor. The reactor was a Pyrex-glass U-tubing with 0.003 m i. d., in which either 0.1 g of the doped powdered catalyst or 0.2 g of the supported catalyst was packed and fixed with two glass wool beds. The reactor part is shown in Fig. 1. The five way tap was equipped with a sample loop 1.59 ml capacity. One side of the loop was connected through a three way tap, to the vacuum system equipped with

reactant gas reservoirs. A standard reactant mixture of 3% C_2H_4 , 20% O_2 , and 77% He by volume was prepared using purified gases. Pulse size of the reactant mixture was 0.25 ml (STP) and pulse interval was 14 min. The catalyst packed in the reactor was again reduced in the stream of H_2 at 673 K for 20~60 min, and cooled to the reaction temperature. Analysis of the products was performed by a gas chromatograph. $\text{C}_2\text{H}_4\text{O}$ was separated in a DOP column and O_2 , CO_2 , and C_2H_4 by a Porapack Q column. The two columns were connected in series via a thermal conductivity detector. After a set of pulse reactions at a given temperature, the catalyst were always reduced by H_2 at the subsequent reaction temperature for 15 min.

The specific surface area was determined by BET method. Bulk composition of catalyst was measured at room temperature by XRD (CuK_α , 35 kV, 25 mA). As an internal standard, 0.1 g of $\alpha\text{-Al}_2\text{O}_3$ was used and mixed well with 0.4 g of catalyst sample.

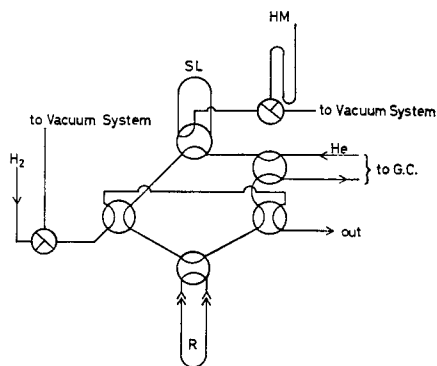


Fig. 1. Schema of reactor part,

- SL: Sample loop,
- HM: Hg-vacuum manometer,
- R: Fixed bed reactor.

X-ray photoelectron spectrometer (MgK_{α} , 1253.6 eV) used was ESCA3 (VG) with a base pressure of 10^{-10} torr level. AES (VG) was another separate instrument. Binding energy was calibrated using C 1s peak centred at 284.6 eV. The doped, powdered sample was pressed on a net of gold wire spot-welded on the sample holder made of nickel metal. Immediately before inserting the samples into the spectrometer, they were in situ treated in H_2 at atmospheric pressure and at 673 K overnight in the preparation chamber. After the treatment, the cycles of outgassing, reducing, and annealing were carried out. All recordings of AES and XPS measurements were done at 295 K.

Results

Pulse Reaction

Activity, represented as $\text{C}_2\text{H}_4\text{O}$ formation rate, r_{EO} , and as $\text{C}_2\text{H}_4\text{O}$ concentration in the gaseous part of the product, $(\text{EO})_{\text{EO}}$, are shown in Figs. 2 and 3. The results were obtained using the standard reaction gas mixture. The rate of $\text{C}_2\text{H}_4\text{O}$ formation was determined in a differential reactor since the pseudo-first order kinetics¹²⁾ was established. The activity and selectivity for the pure silver catalyst prepared by the same preparation procedure as for the NaCl-doped catalyst are shown in Table 1 for comparison. In Fig. 4, the drop in catalytic activity between 1st and 2nd pulses is noticeable, but only slight decrease is between 2nd and 4th pulse. However, discrepancy in carbon balance was observed in each pulse reaction. The discrepancy showed a similar dependence on pulse number as the activity. In the 1st

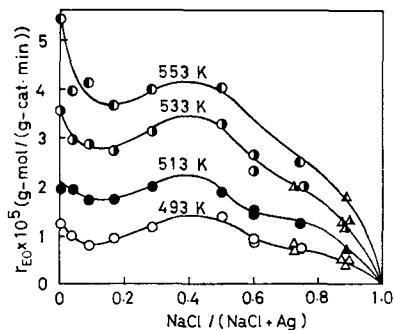


Fig. 2. Dependences of $\text{C}_2\text{H}_4\text{O}$ formation rate on NaCl content,

Circle marks: Doped catalysts,
Triangle marks: Supported catalysts.

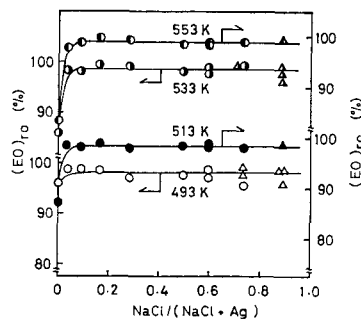


Fig. 3. Dependences of $\text{C}_2\text{H}_4\text{O}$ concentration in the gaseous part of the product.

Circle marks: Doped catalysts,
Triangle marks: Supported catalysts.

Characteristics of Silver Catalysts

TABLE 1. Catalytic Activity and Selectivity of Pure Silver Powdered Catalyst*

Reaction Temperature (K)	Total Formation Rate (mol/g-cat min) $\times 10^5$	Selectivity (%)
413	2.79	43.3
423	4.31	32.1
433	6.15	30.9
444	8.32	30.0

* No changes in activity and selectivity with pulse number were observed.

pulse reaction just after the hydrogen reduction at 473~673 K, about 12% of C_2H_4 injected was lost and the amount was almost independent of reaction temperature and NaCl content. In the 2nd to 4th pulses, the carbon balance discrepancy was ~4%. However, products other than C_2H_4O , CO_2 and H_2O were not detected. Therefore, in the present work, the average values of 2nd to 4th pulse reactions are used to evaluate the activity and selectivity.

As seen from Figs. 2 and 3, the doped catalysts are active for the epoxidation in the wide range of NaCl content and the activity decreases moderately through a maximum in the middle range NaCl content, although the activity is low in comparison with pure silver (Table 1). The C_2H_4O concentration is very high (97~99%) and almost independent of NaCl content at all temperatures studied except for 0.001 NaCl-doped catalyst, where the value of 0.001 implies the ratio of NaCl to Ag in equivalent weight. The supported catalysts exhibited comparable activity and $(EO)_{ro}$ to those of the doped catalysts, as seen from the data shown by triangle marks in Figs. 2 and 3.

The C_2H_4O formation rate increased with increasing $P_{C_2H_4}$ and P_{O_2} . However, a saturation limit is observed with $P_{O_2} \geq 0.08$ atm. The C_2H_4O concentration increases with decreasing $P_{C_2H_4}$ or increasing P_{O_2} , as seen from Figs. 5 and 6. It was however difficult to evaluate the exact rate of CO_2 formation because the amount of CO_2 produced was small.

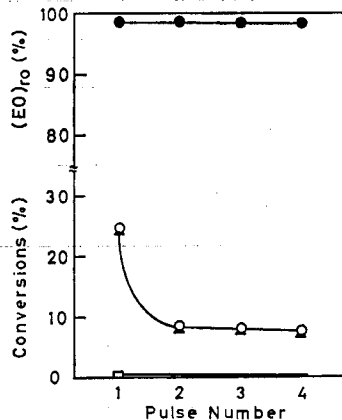


Fig. 4. Variations of conversions and C_2H_4O concentration in the product with pulse number at 513 K for 0.04 NaCl-doped catalyst,
 ○ : Total conversion,
 ▲ : Conversion to C_2H_4O ,
 □ : Conversion to CO_2 ,
 ● : C_2H_4O concentration.

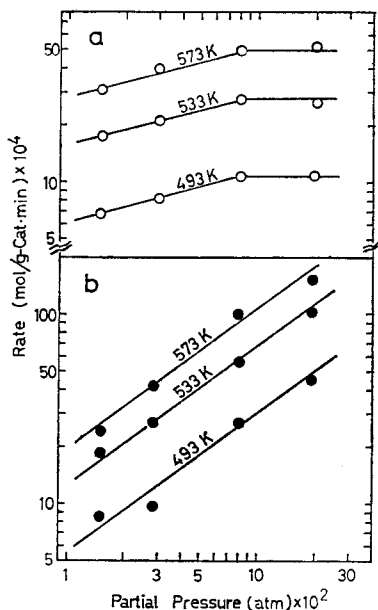


Fig. 5. Dependences of C_2H_4O formation rate (r_{EO}) on p_{O_2} at $p_{C_2H_4}$ 0.03 atm (a) and on $p_{C_2H_4}$ at p_{O_2} 0.20 atm (b) over 0.04 NaCl-doped catalyst.

Oxidation of Ethylene Oxide

The oxidation of C_2H_4O was carried out over 0.04 NaCl-doped catalyst and 2.8 NaCl-supported catalyst, using the reactant mixture of 3% C_2H_4O , 20% O_2 , and 77% He by volume (Fig. 7). The conversion of C_2H_4O to CO_2 was only 0.07% at 533 K for 0.04 NaCl-doped catalyst, while for 2.8 NaCl-supported catalyst the conversion was nearly zero even at 573 K. Other products were not detected. However, 14~23% of injected C_2H_4O was lost during the reaction on both the catalysts. The loss was larger than that observed in the oxidation of C_2H_4 over the same catalysts, and was also independent of the reaction temperature.

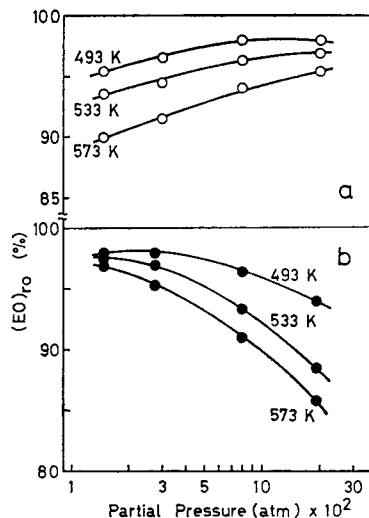


Fig. 6. Dependences of C_2H_4O concentration in the product on p_{O_2} at $p_{C_2H_4}$ 0.03 atm (a) and on $p_{C_2H_4}$ at p_{O_2} 0.20 atm (b) over 0.04 NaCl-doped catalyst.

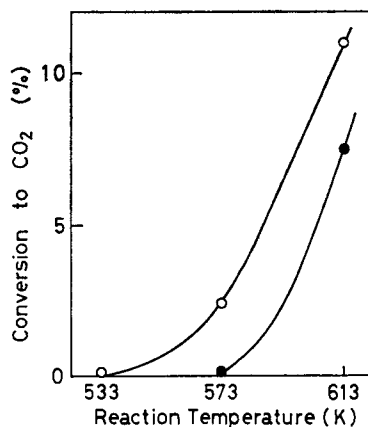


Fig. 7. Changes in conversion of C_2H_4O to CO_2 with reaction temperature (C_2H_4O : 3 vol %, O_2 : 20 vol %),
 ○ : 0.04 NaCl-doped catalyst (0.1 g),
 ● : 2.8 NaCl-supported catalyst (0.2 g).

Characteristics of Silver Catalysts

Surface Area

The surface areas of the doped catalysts were in the range of 0.22 to 0.40 $\text{m}^2 \text{g}^{-1}$, and those of powdered NaCl and the pure silver were 0.14 and 0.26 $\text{m}^2 \text{g}^{-1}$, respectively (Fig. 8). The catalysts consisting of Ag and NaCl in the equivalent weight ratio of 1:0.1~0.3 were very fine powder.

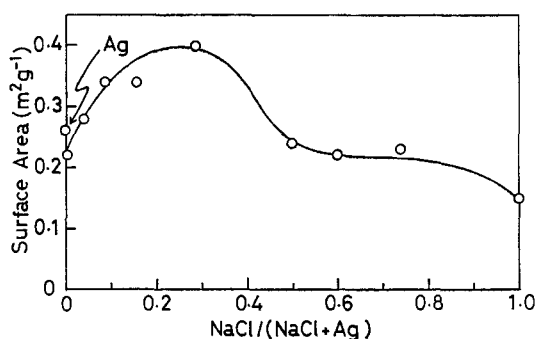


Fig. 8. Relation between surface area and NaCl content.

Annealing Effect

Fig. 9 shows the variations of activity, the $\text{C}_2\text{H}_4\text{O}$ concentration, and surface area with temperature, when 0.04 NaCl-doped catalyst was treated in H_2 at atmospheric pressure for 10 h. Also, for the 2.8 NaCl-supported catalyst the activity and selectivity remained unchanged up to 843 K. These results show the excellent thermal stability of the catalysts containing Ag and NaCl.

XRD

When the powdered Ag_2O was mixed with an aqueous solution of NaCl, AgCl was, of course, immediately formed. In the case of large amount of NaCl, the color of the precipitated mixture was whitish light-violet. However, the dried mixture was the same dark brown colour as Ag_2O . XRD measurements showed that the mixture consisted of only Ag_2O , NaCl, and AgCl. No Ag and NaOH were dedected.

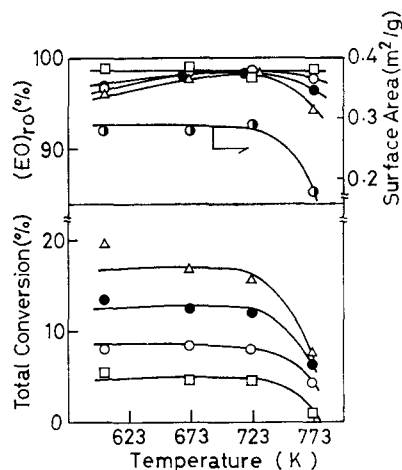


Fig. 9. Variations in total conversion, $\text{C}_2\text{H}_4\text{O}$ concentration, and surface area with annealing temperature in a stream of H_2 for 10 h (0.04 NaCl-doped catalyst),
Reaction temperature:
○ : 493 K, □ : 513 K,
● : 533 K, △ : 553 K.

A. AYAME, *et al.*

The complete reduction of Ag_2O and AgCl in the mixture was not attained by treating in a stream of H_2 at 333 K for 20 h or more. When the precipitate was exposed at different temperatures to H_2 , the bulk composition exhibited remarkable changes, as shown in Fig. 10. The relative intensity implies the intensity ratio of the most intense XRD peak of each component to that of $\alpha\text{-Al}_2\text{O}_3$ at 35.2° (2θ), in the case of Ag the intensity of (200) peak at 44.3° is used because the Ag(111) peak at 38.7° coincides with Ag_2O (200) peak. The treatment of the sample was performed by elevating its temperature at 2-hour intervals in a stream of H_2 . A part (Ca.

0.4 g) of the sample treated at a given temperature was taken out of the tube, mixed well with the internal standard, and then measured by XRD. The reduction of Ag_2O in the mixture proceeded in the temperature interval 373 to 573 K, and the rapid reduction of AgCl was observed above 523 K. Further, the peak of Ag_2O was detected until AgCl peak was completely eliminated. The treatment at 673 K for 2 h or more converted the mixture to solely Ag and NaCl.

AES and XPS

The surfaces of pure Ag powder and that of 0.5 NaCl-doped catalysts were characterized by AES. Fig. 11 compares Auger spectra measured at 295 K. The observed four Ag peaks at 266, 304, 351, and 356 eV agree with those for standard metallic Ag.¹³⁾ For the Ag powder, the C peak at 272 eV is negligible small and the intensity ratio of Ag peaks at 266 eV and 304 eV is 0.55. Consequently, the surface of the Ag powder is almost clean,³¹⁾ which is also ascertained by XPS spectrum of C 1s (Fig. 12). For the 0.5 NaCl-doped catalyst, although the intensity ratio of Ag 266 eV to Ag 304 eV peak is 0.8 and the C 272 eV peak emerges clearly, XPS peak of C 1s is very small. AES peaks at 181, 503, and 990 eV are assigned to Na, O, and Cl, respectively. No other peaks were observed. From these results, it is obvious that the catalyst surface is contaminated with oxygen and small amount of amorphous carbon.²⁹⁾

Fig. 13 shows Ag $3d_{5/2}$ XPS spectra for both the samples. For the

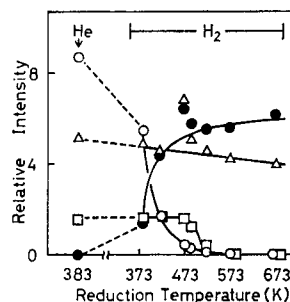


Fig. 10. Change of the bulk composition of 1.0 NaCl-doped catalyst with reduction temperature as deduced by XRD. The relative intensity means the ratio of the intensity of a given XRD peak to that at $2\theta=35.2^\circ$ for $\alpha\text{-Al}_2\text{O}_3$.

○ : Ag_2O (32.7°), △ : NaCl (31.7°),
 □ : AgCl (32.2°), ● : Ag (44.3°).

Characteristics of Silver Catalysts

Ag powder, the binding energy of Ag $3d_{5/2}$ peak is 368.2 eV and the FWHM 1.1 eV. However, for the NaCl-doped catalyst, Ag $3d_{5/2}$ peak is broadened (FWHM 1.3 eV) and a new shoulder around ~ 369.5 eV emerges. Such a

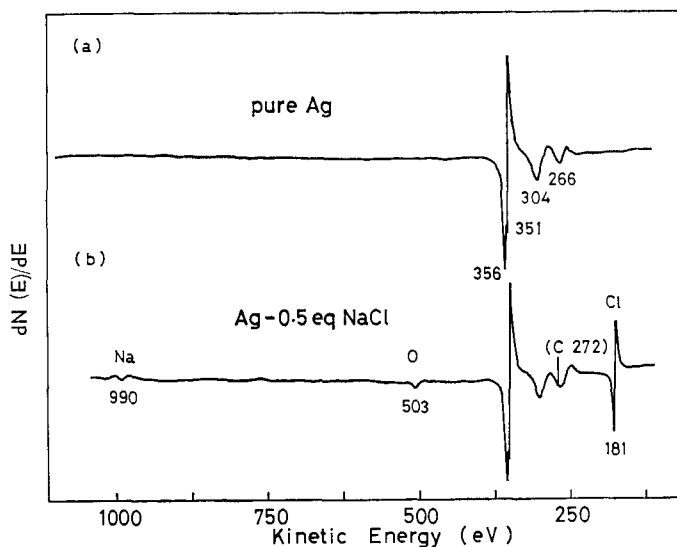


Fig. 11. Auger spectra of pure silver powder and 0.5 NaCl-doped catalyst.

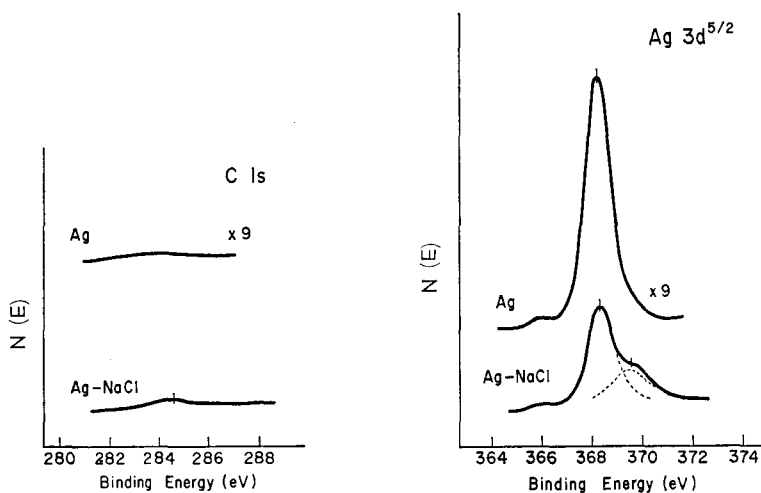


Fig. 12. XPS spectra of C 1s region for pure silver powder and 0.5 NaCl-doped catalyst (10^3 c/s).

Fig. 13. XPS spectra of Ag $3d_{5/2}$ region for pure silver powder and 0.5 NaCl-doped catalyst (10^4 c/s).

A. AYAME, *et al.*

splitting was also observed in the Ag $3d_{3/2}$ peak in a similar manner. The XPS spectra of Na 1s, Cl 2p, and O 1s regions are also shown in Fig. 14. The Na 1s spectrum splits into two peaks at 1073.0 and 1075.8 eV. Also, the Cl 2p spectrum is a broad peak centered at 201.9 eV having a shoulder at 198.9 eV. Further, XPS spectrum of O 1s region consists of three peaks at 532.0, 533.3, and 534.5 eV and the FWHM is very large.

Discussion

As stated earlier, the commercial silver catalysts include small amounts of alkali or alkaline earth metals and trace amounts of chlorine-containing organic compounds are also added into reactant gas streams. In the course of our work on the effects of simultaneous inclusion of the both elements—*i.e.* one of the alkali metals and chlorine— into silver catalyst, it has been found that the silver catalysts including equimolecular sodium and chlorine exhibit the characteristic behaviors for the epoxidation of ethylene. Since NaCl is essentially inactive for the epoxidation, the activity change with increasing NaCl content seems to be attributable to variations in the physico-chemical property of Ag particles or atoms, which is caused by the strong chemical interactions of Ag with NaCl (or Na^+ , Cl^-) and adsorbed oxygen. The activity and selectivity were drastically modified with doping only 0.001 equivalent of NaCl to Ag.

The pattern of variation of activity of the NaCl doped catalysts with increasing NaCl content is however, complex (Fig. 2). The $\text{C}_2\text{H}_4\text{O}$ formation rate, r'_{EO} , when referred solely to weight of Ag increases monotonously with NaCl content (Fig. 15). This result implies that Ag particle is highly dispersed on the surface with increasing NaCl content. This speculation is supported by the fact that the activity of the NaCl-supported catalyst is comparable to that of doped catalyst with the same NaCl content (Figs. 2, 3, and 15), and to that of the reduced catalysts consisting of only Ag and NaCl (Fig. 10).

The $\text{C}_2\text{H}_4\text{O}$ concentration of 97~99% in the gaseous product obtained in this study is very high, but about 4% of C_2H_4 injected was irreversibly adsorbed and remained on the catalyst. On silver catalysts after use for

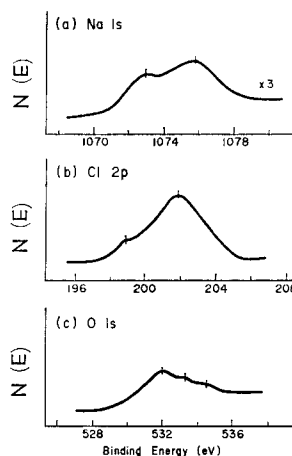


Fig. 14. XPS spectra of Na 1s, Cl 2p, and O 1s regions for 0.5 NaCl-doped catalyst (10^3 c/s).

Characteristics of Silver Catalysts

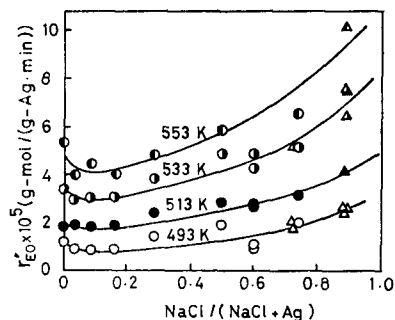


Fig. 15. Relationship between C₂H₄O formation rate referred to weight of Ag and NaCl content at different temperatures.

Circle marks: Doped catalysts,
Triangle marks: Supported catalysts.

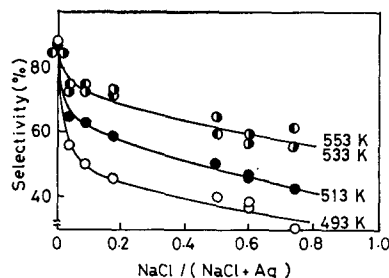


Fig. 16. Relation between selectivity and NaCl content obtained over the doped catalysts, when the lost C₂H₄ is assumed to be converted to CO₂ and H₂O finally.

ethylene oxidation, oxygen-containing hydrocarbons or polymerlike materials,^{14-16,18)} and combustion intermediates¹⁶⁻¹⁸⁾ have been reported to exist. However, in the case of Ag-NaCl catalysts, the material remained seems to be strongly held on the catalyst surface as CO₂ or its precursors, because the effusion of CO₂ together with H₂O was observed on exposing the used catalysts to a stream of H₂. The effused H₂O could be due to the reduction of adsorbed oxygen. Assuming that the C₂H₄ lost remains on the catalyst as CO₃²⁻ or converts to CO₂ and H₂O finally, the true selectivity to C₂H₄O decreases with increasing NaCl content, as shown in Fig. 16. The higher selectivity at elevated temperatures can not be predicted from a general relationship between selectivity and reaction temperature for complex reactions. However, this result could be inferred from the increase in the amount of the enhanced adsorption of CO₂ or its precursors with lowering temperature.

Only the 0.001 NaCl-doped catalyst gave a good carbon balance and normal relation of selectivity to temperature, in a similar manner to pure silver. Then, the catalyst showed 84~87% selectivity, which agreed with those measured over several NaCl-doped catalysts using a reductive reactant gas mixture.¹⁰ The selectivity is also corresponding to the maximum expected by the mechanism proposed by Kilty and Sachtler.³⁾ Sodium cations incorporated in the catalysts are probably responsible for the enhanced adsorption of CO₂ or its precursors.

From the kinetic data in Fig. 5, the following rate equations were obtained :

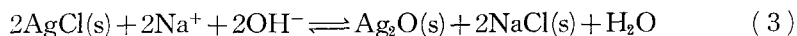
A. AYAME, *et al.*

$$\begin{aligned} &\text{At } p_{\text{O}_2} \leq 0.08 \text{ atm,} \\ &r_{\text{EO}} = 13.5 \exp(-43,900/RT) P_{\text{C}_2\text{H}_4}^{0.74} P_{\text{O}_2}^{0.25} \end{aligned} \quad (1)$$

$$\begin{aligned} &\text{At } p_{\text{O}_2} \geq 0.08 \text{ atm,} \\ &r_{\text{EO}} = 7.5 \exp(-43,900/RT) P_{\text{C}_2\text{H}_2}^{0.74} \end{aligned} \quad (2)$$

where R is gas constant ($\text{JK}^{-1}\text{mol}^{-1}$). The apparent activation energy agrees with $42\sim 55 \text{ KJ mol}^{-1}$ estimated from data shown in Fig. 2 and is less than those reported in literature.^{14,15,19~22)} Also, the fractional reaction order might suggest that the epoxidation proceeds through Langmuir-Hinshelwood type mechanism. The high thermal stability of Ag-NaCl catalysts was evidenced by the effects of calcination (Fig. 9). The crystallite size of Ag when annealed at 673 K was about 420 Å and is larger than that observed for pure Ag. These results mean that Ag particles have been aggregated at lower reduction temperatures by the strong interaction of Ag and NaCl. The elevation in selectivity and the decrease in activity with aggregating Ag particles have been reported by many workers.³⁰⁾

The variation of bulk composition in the course of catalyst preparation is an interesting phenomenon. Especially, the variation after drying the precipitated mixture must be caused by a solid phase reaction. $\text{Ag}_2\text{O-K}_2\text{SO}_4$ mixture and pure Ag_2O were completely reduced by H_2 at 323~373 K for 20 h.^{16,17)} Comparing with these results, the reduction temperature of the NaCl-doped catalysts is shifted to higher temperatures. In the dried mixture, the following equilibrium would have been established.



where most of Na other than NaCl is present in cationic form with equivalent amount of OH^- , since no XRD peaks of NaOH crystal were detected and the mixture was not completely dehydrated. In such a situation, we believe that Na_2O can not exist because Na_2O is thermodynamically less stable than NaOH. The qualitative composition of the dried mixture determined by XRD corresponds to an equilibrium state. The slower disappearance of Ag_2O XRD peaks than AgCl with increasing temperature (Fig. 10) suggests that AgCl is converted thermally to Ag_2O , and then reduced by H_2 . This has been ascertained by the result that when the precipitate was heated in a stream of He at atmospheric pressure upto 673 K, the reaction of Eq. (3) took place in the same manner as shown in Fig. 10.²⁰⁾

According to AES spectrum in Fig. 11-(b), it is speculated that distribution of each element in the bulk is not uniform; the surface concentration of elements, calculated from the relative intensities of AES peaks, is 1 : 0.6 :

Characteristics of Silver Catalysts

2.2 : 0.1 for Ag : Na : Cl : 0. Comparing with the original composition of the catalyst, it is noted that Cl and Na concentrate on the surface layers.

The binding energy of 368.3 eV for Ag 3d_{5/2} and the separation due to spin-orbit splitting for the silver powder agreed with those reported by Romand *et al.*²⁴⁾ The FWHM of 1.1 eV of Ag 3d_{5/2} was smaller than 1.3 eV reported by Romand *et al.*, but rather near to 1.15 eV for silver metal.²⁵⁾ The binding energy and the spin-orbit energy separation for the 0.5 NaCl-doped catalyst were almost the same as for the pure Ag powder. However, Ag 3d_{5/2} peak broadened and a new peak (or shoulder) developed (Fig. 13). At the same time, Ag 4d doublet peak broadened at the higher binding energy side. Zatko nad Prather²⁶⁾ reported that Ag³⁺ of diamagnetic ethylenedis (biguanide) silver (III) persulfate gave an Ag 3d_{5/2} peak at 371.4 eV. Romand *et al.*²⁴⁾ indicated that the difference in binding energy of Ag 3d between Ag and Ag₂O was only +0.1 eV and the FWHM for Ag₂O was larger than for Ag. Consequently, the new peak at about 369.5 eV seems to correspond to a higher oxidation state of Ag other than Ag⁺, and the 368.3 eV peak may include an effect of the presence of Ag⁺ because of spreading of +0.2 eV in its FWHM.

In order to compare with the Na 1s and Cl 2p XPS spectra in Fig. 14, the spectra for pure NaCl were measured (4.0 eV charging-up was observed). The binding energies of Na 1s and Cl 2p_{3/2} peaks were 1072.4 eV (FWHM 2.2 eV) and 198.3 eV (FWHM 2.6 eV), respectively, and the Na 1s-Cl 2p_{2/3} peak separation was 874.1 eV. Comparing these results with those obtained for the 0.5 NaCl-doped catalyst, *i. e.* the Na 1s peak at 1073.0 and the Cl 2p_{3/2} peak at 198.9 eV were similar to their original peaks and the peak separation was of the same value. In general, Na 1s is a singlet, Cl 2p a doublet, and Cl 2p_{3/2} has higher intensity, nearly equal to 3/2 of Cl 2p_{1/2}. Consequently, the 1075.8 eV peak of Na 1s and the 201.9 eV peak of Cl 2p in Fig. 14 are new ones, which seems to be related to the emergence of the 369.5 eV peak of Ag 3d_{5/2}. The peak separation between the new peak at the high binding energy side and its original peak for Ag 3d, Na 1s, or Cl 2p were 1.2, 2.8, or 3.0 eV, respectively. If the so called "charging-up" is responsible for the shifts, an equal separation should be observed for each of the atoms. Further, large shifts for Na 1s and Cl 2p can not be found in literature, except for Cl 2p_{3/2} at 206 and 208 eV for KClO₃ and CsClO₄, respectively.²⁵⁾ The assignments of the peaks at the high binding energy side will be the subject of future studies by us. The fact that the values of FWHM for Ag 3d_{5/2}, Na 1s, and Cl 2p spectra for the doped catalyst were larger than those of pure Ag reflects the spreads or distortions of their

band structures.

When oxygen was adsorbed on pure silver at 295 K, three O 1s peaks at 530.0, 531.3, and 533.5 eV have been observed, and these peaks, were assigned respectively to surface oxygen atom, subsurface oxygen atom, and oxygen admolecule.²⁷⁾ Thereby, the largest O 1s peak at 532.0 eV in Fig. 14-(c) is assigned to subsurface oxygen atom, and the 533.3 peak to oxygen admolecule.²⁸⁾ The peak at 534.5 eV would be related to the appearance of the Ag 3d_{5/2} 369.5 eV peak, but its details are uncertain. The O 1s spectrum and AES peak of oxygen were not eliminated even after several times of overnight in situ reduction at 673 K in the preparation chamber. Even at 673 K, the XPS spectrum due to subsurface oxygen was observed. It was, therefore, speculated that small amount of oxygen is confined in the surface layers by strong ionic interactions with Ag, Na, and Cl. The concentration ratio of oxygen to Ag was about 0.1 as deduced from the AES spectrum.

In a separate study it has been shown that most of the oxygen adsorbed on the NaCl-doped catalysts at 373~673 K exhibited irreversible behaviour (Table 2), and are less active for the epoxidation of C₂H₄.²⁹⁾ The irreversibly adsorbed oxygen seems to correspond to the subsurface oxygen atom. Such an oxygen atom would function as a direct or indirect active site in the subsequent oxygen adsorption and epoxidation of C₂H₄. Finally, it is deduced that the existence of NaCl in silver catalyst causes the spreading of band structure of Ag thus leading to the formation of its higher oxidation states and, at the same time, the band structures of Na and Cl are distorted. The distortions of their band structures are promoted by the presence of subsurface oxygen.

TABLE 2. The total and irreversible amount of oxygen adsorbed on the NaCl-doped catalysts. (by the gas chromatographic method using a stream of helium including oxygen at 1.15×10^{-2} atm)

Catalyst	NaCl-content*	Amount of Adsorbed Oxygen (mℓ/g-cat)			
		at 353 K		at 473 K	
		Total	Irr.**	Total	Irr.**
Ag-NaCl	0.4	0.013	0.011	0.026	0.017
	1.0	0.019	0.018	0.039	0.029

* Mole ratio of NaCl to Ag.

** Irreversibly adsorbed oxygen.

Characteristics of Silver Catalysts

Acknowledgment

The authors are grateful to Mr. Akira Tejima of Muroran Institute of Technology for his valuable help in building up of the glass apparatus. This work was generously supported by a grand-in-Aid for Scientific Research (No. 56470062) from the Ministry of Education of Japan (KM and IT).

References

- 1) T. E. Lefort, Fr. Patent, 729952.
- 2) L. Ya. Margolis, *Advanced in Catalysis*, vol. 14, p. 429. Academic Press, New York, 1963; H. H. Voge and C. R. Adams, *Advanced in Catalysis*, vol. 17, p. 151, 1967; T. Seiyama, *Kagaku to Kogyo*, **21**, 1002 (1968); W. M. H. Sachtler, *Catal. Rev.*, **4**, 27 (1970); D. J. Hucknall, *Selective Oxidation of Hydrocarbon*, p. 6, Academic Press, London and New York, 1974; A. Ayame and H. Kanoh, *Shokubai, (Catalyst)* **20**, 381 (1978); N. Nojiri, *Petrotech*, **1**, 598 (1978); X. E. Verykios, F. P. Stein and R. W. Coughlin, *Catal. Rev. Sci. Eng.*, **22**, 197 (1980); W. M. H. Sachtler, C. Backx and R. A. VanSanten, *Catal. Rev. Sci. Eng.*, **23**, 127 (1981).
- 3) P. A. Kilty and W. M. H. Sachtler, *Catal. Rev. Sci. Eng.*, **10**, 1 (1974); P. A. Kilty, N. C. Rol and W. M. H. Sachtler, *Pap. 64*, 5th Int. Congr. Catal., Palm Beach, 1972.
- 4) U. S. Patent, 2426721.
- 5) Jpn. Patents, 49-30286; 50-74589; 51-36245; 50-90591; 52-151690; 53-1191.
- 6) V. E. Ostrovskii, N. V. Kul'kova, V. L. Lapatin and M. I. Temkim, *Kinet. Catal.*, **3**, 160 (1962).
- 7) H. T. Spath, *Pap. 65*, 5th Int. Congr. Catal., Palm Beach, 1972.
- 8) E. L. Foce and A. T. Bell, *J. Catal.*, **44**, 175 (1976).
- 9) H. T. Spath, G. S. Tomazic, H. Wurm and K. Torkar, *J. Catal.*, **26**, 18 (1972).
- 10) L. Pauling, *The Nature of the Chemical Bond (3rd Ed.)*, p. 351, Cornell Univ. Press, Ithaca, New York, 1960.
- 11) A. Ayame, N. Takeno and H. Kanoh, *J. C. S. Chem. Comm.*, **1982**, 617.
- 12) D. W. Bassett and H. W. Habgood, *J. Phys. Chem.*, **64**, 769 (1960).
- 13) *Handbook of Auger Electron Spectroscopy (2nd Ed.)*, Phys. Electronic Div., Perkin-Elmer Corp., Minnesota.
- 14) G. H. Twigg, *Proc. Roy. Soc. London*, **A188**, 92 (1946).
- 15) A. Orzechowski and K. E. MacCormack, *Can. J. Chem.*, **32**, 388 and 432 (1954).
- 16) A. Ayame, A. Numabe, Y. Watanabe and H. Kanoh, *Nippon Kagaku Kaishi*, **1973**, 2071; A. Ayame, A. Numabe, T. Kanazuka and H. Kanoh, *Bull. Jpn. Petrol. Inst.*, **15**, 142 (1973).
- 17) M. Kobayashi, M. Yamamoto and H. Kobayashi, *Pap. A 24*, 6th Int. Congr. Catal., London, 1976; M. Kobayashi and H. Kobayashi, *J. C. S. Chem. Comm.*, **1977**, 71.
- 18) A. Ayame, Y. Shibuya, T. Yoshida and H. Kanoh, *Nippon Kagaku Kaishi*, **1973**, 2063.

A. AYAME, *et al.*

- 19) A. Ayame, H. Kanoh, T. Kanazuka and H. Baba, *Bull. Jpn. Petrol. Inst.*, **15**, 150 (1973).
- 20) Sh. W. Wan, *I & EC.*, **45**, 234 (1953).
- 21) S. Hartwig and J. Bathory, *Zeit. Physiki. Chem.*, **55**, 208 (1967).
- 22) R. E. Kenson and M. Lapkin, *J. Phys. Chem.*, **74**, 1493 (1970).
- 23) M. Yamaguchi and A. Ayame, Unpublished.
- 24) M. Romand, M. Roubin and J. P. Deloume, *J. Electron Spectrosc. Relat. Phenom.*, **13**, 229 (1978).
- 25) *Handbook of X-ray Photoelectron Spectroscopy*, Phys. Electronic Div., Perkin-Elmer Corp., Minnesota.
- 26) D. A. Zatko and J. W. Prather II, *J. Electron Spectrosc. Relat. Phenom.*, **2**, 191 (1973).
- 27) H. Miura, A. Ayame, H. Kanoh, K. Miyahara and I. Toyoshima, *Shinku (Vacuum)*, **25**, 147 (1982).
- 28) R. W. Joyner and M. W. Roberts, *Chem. Phys. Lett.*, **60**, 459 (1979); M. W. Roberts, *Advanced in Catalysis*, Vol. 29, 55 (1980).
- 29) M. G. Mason and R. C. Baetzold, *J. Chem. Phys.*, **64**, 271 (1976).
- 30) For example; J. C. Wu and P. Harriott, *J. Catal.*, **39**, 395 (1975); H. Kanoh, T. Nishimura and A. Ayame, *J. Catal.* **57**, 372 (1979); A. E. B. Presland, G. L. Price and D. L. Trimm, *J. Catal.*, **26**, 313 (1972).
- 31) S. R. Keleman and I. E. Wacks, *Surf. Sci.*, **97**, L 370 (1980).